

Charge separation and temperature-induced carrier migration in $\text{Ga}_{1-x}\text{In}_x\text{N}_y\text{As}_{1-y}$ multiple quantum wells

T. Nuytten*

Institute for Nanoscale Physics and Chemistry (INPAC), K.U. Leuven, Celestijnenlaan 200D, B-3001 Leuven, Belgium

M. Hayne

Department of Physics, Lancaster University, Lancaster LA1 4YB, United Kingdom

Bhavtosh Bansal

*Department of Physical Sciences, Indian Institute of Science Education and Research (IISER) Kolkata, Mohanpur, Nadia 741252, India*H. Y. Liu[†] and M. Hopkinson*Department of Electronic and Electrical Engineering, University of Sheffield, Mappin Street, Sheffield S1 3JD, United Kingdom*

V. V. Moshchalkov

Institute for Nanoscale Physics and Chemistry (INPAC), K.U. Leuven, Celestijnenlaan 200D, B-3001 Leuven, Belgium

(Received 16 December 2009; revised manuscript received 7 March 2011; published 5 July 2011)

We have investigated the photoluminescence (PL) of two carefully selected dilute nitride $\text{Ga}_{1-x}\text{In}_x\text{N}_y\text{As}_{1-y}$ multiple quantum well structures in magnetic fields up to 50 T as a function of temperature and excitation power. The observation of a nonmonotonic dependence of the PL energy on temperature indicates that localized states dominate the luminescence at low temperature, while magneto-PL experiments give new insights into the nature of the localization. We find that the low-temperature spatial distribution of carriers in the quantum well is different for electrons and holes because they are captured by different disorder-induced complexes that are spatially separated. A study of the thermalization of the carriers toward free states leads to the determination of the free-exciton wave-function extent in these systems and enables an assessment of the localization potentials induced by inhomogeneity in the quantum well.

DOI: [10.1103/PhysRevB.84.045302](https://doi.org/10.1103/PhysRevB.84.045302)

PACS number(s): 78.67.De, 73.21.Fg, 78.55.Cr

I. INTRODUCTION

The incorporation of a few percent of nitrogen in semiconductor quantum wells (QWs) has recently proven to be a valuable approach in reaching long wavelength emission for GaAs-based telecommunication systems.¹⁻³ In particular, the presence of a small amount of nitrogen in the $\text{In}_x\text{Ga}_{1-x}\text{As}$ alloy causes a dramatic redshift of the host material band gap and an increased insensitivity of the band gap energy to temperature T .⁴ However, fabrication of high-quality $\text{Ga}_{1-x}\text{In}_x\text{N}_y\text{As}_{1-y}$ -based 1.55- μm devices remains a difficult task due to a large miscibility gap, which in turn results in an increased tendency for phase separation and strong carrier localization.^{5,6}

In the present work we use magneto-photoluminescence (magneto-PL) to study carrier localization in two contrasting samples: one grown at an elevated temperature and without lattice matching between the QWs and the barrier material, and one with optimized growth temperature and sample morphology. We build up a consistent phenomenological picture of the localization of electrons and holes in these two samples.

The paper is organized as follows. In Sec. II we summarize the growth details of the two samples under consideration, describe the experimental setup, and introduce the model we have used to analyze the data. Section III presents the temperature dependence of the PL spectra in the absence of a magnetic field B , as well as the temperature dependent magneto-PL, which are discussed further in Sec. IV. In Sec. V we conclude.

II. SAMPLE DETAILS AND EXPERIMENTAL SETUP

The samples in this study, labeled A and B, were grown on (001) GaAs substrates by molecular beam epitaxy with nitrogen incorporated using a radio-frequency plasma source.⁶⁻⁸ The active region for Sample A was grown at 460 °C and consists of a 52 nm $\text{GaN}_{0.007}\text{As}_{0.993}$ barrier layer followed by five 8-nm $\text{Ga}_{0.65}\text{In}_{0.35}\text{N}_{0.023}\text{As}_{0.977}$ QWs between $\text{GaN}_{0.007}\text{As}_{0.993}$ spacer layers and another $\text{GaN}_{0.007}\text{As}_{0.993}$ barrier layer. Sample B, grown at 325 °C, has the same structure but has three $\text{Ga}_{0.62}\text{In}_{0.38}\text{N}_{0.03}\text{As}_{0.97}$ QWs between $\text{Ga}_{0.977}\text{In}_{0.023}\text{N}_{0.01}\text{As}_{0.99}$ barriers. The $\text{GaN}_{0.007}\text{As}_{0.993}$ barriers in Sample A are tensile strained and thus act as strain-compensating layers to the compressively strained QWs, while the small addition of indium to the barrier material in Sample B reduces the strain at the QW-barrier interface and improves the optical and structural properties of the QW.^{6,9} PL spectra were obtained in a He bath and a He flow cryostat at temperatures between 4.2 and 200 K, located in the bore of either a homemade pulsed field coil or a DC superconducting 12 T magnet. Magnetic field pulses of 20 ms and up to 50 T were generated using a 5-kV, 500-kJ capacitor bank. In both setups the sample was mounted with the magnetic field applied in the growth direction, and excitation from a solid-state laser at 532 nm was delivered perpendicular to the sample surface via a 200- μm core optical fiber. Excitation power densities ranged over six orders of magnitude, between 5×10^{-5} and 50 Wcm^{-2} . The luminescence was collected by a second

optical fiber and analyzed using a 30-cm monochromator and a liquid-nitrogen-cooled InGaAs diode array, recording several PL spectra during each field pulse.

The dependence of the center of mass of the PL energy (hereafter referred to as PL energy) E_{cm} , on magnetic field B , is analyzed using an excitonic model in which it is assumed that there is a critical magnetic field

$$B_c = \frac{2\hbar}{e\langle\rho^2\rangle}, \quad (1)$$

where the field dependence of the PL energy passes smoothly from a low-field regime, in which there is a parabolic B dependence, to a high-field regime, in which there is a linear B dependence.¹⁰ In the above equation e is the charge of the electron, \hbar the reduced Planck constant and $\langle\rho^2\rangle^{1/2}$ the average exciton wave-function extent. Thus, the magnetic field provides a length scale via the magnetic length $\ell_B = \sqrt{\hbar/eB}$ with which to probe the spatial configuration of the excitons. Specifically, it can be seen that the field B_c is reached when $\ell_B = \langle\rho^2\rangle^{1/2}/\sqrt{2}$.

III. RESULTS

In order to investigate the degree of localization in our samples, we have examined the T dependence of the PL energy for both samples (Fig. 1). In agreement with earlier studies,^{8,11–14} a nonmonotonic dependence of the PL energy versus T is observed and is attributed to trapping and subsequent detrapping of carriers by localized states. Electrons and holes created by the nonresonant optical excitation are first trapped in local potential minima closest to the region where they are excited, and then they subsequently migrate to the lower-lying energy minima through a thermally activated process. The PL signal that is observed at a particular T is a result of the competition between the recombination time and the time scale associated with carrier migration to lower energy states closer to the global minimum. Thus at low T , a slight

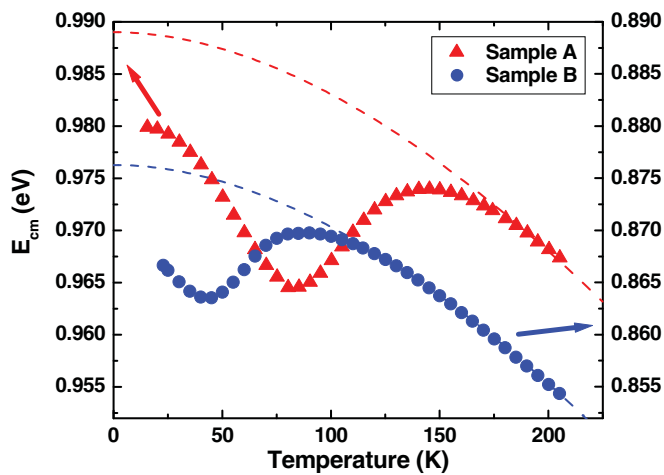


FIG. 1. (Color online) Temperature dependence of the PL energy for samples A (triangles) and B (circles) with an excitation power density of 2.5 Wcm^{-2} . The local minimum in the S shape, typical for recombination from localized states, is more pronounced and appears at higher T for Sample A. Dashed lines indicate the Varshni fits to the high- T data.

increase in temperature thermalizes the carriers, allowing them to reach regions with a higher degree of localization, and we find a sharp redshift with increasing T .

From around 100 K for Sample A and 50 K for Sample B, carriers have enough thermal energy to start to escape the localization, and redistribution toward the higher-energy free-exciton levels begins, causing a decrease in the population ratio between localized and free excitons. This progressive carrier detrapping from the localized states shifts the center of the carrier distribution function toward higher energy. Consequently, the PL signal is increasingly dominated by recombination from free excitons, whose energy levels are higher than the localized levels, and a blueshift is observed. At the highest temperatures (>150 K for Sample A and >100 K for Sample B), a band-gap-like redshift of the PL signal with T is found, showing that radiation from free excitons dominates the PL. Hence, the T dependence of the PL energy has an S shape. The temperature at which the T dependence recovers to a band-gap-like behavior gives an indication of the degree of localization, and in general an increase in nitrogen content in the QW might be expected to increase this temperature. In this case the nitrogen incorporation in Sample B is slightly higher than in Sample A ($x=0.03$ and $x=0.023$, respectively). Despite this, the local minimum of the S shape occurs at higher T for Sample A and is about 50% deeper with respect to Sample B (Fig. 1), testifying to the stronger degree of localization in the sample with the slightly lower N content. This is attributed to other factors related to the sample structure and is discussed below. Note that previous studies have shown that a small difference in nitrogen incorporation does not have a dramatic effect on the properties of the alloy.⁶

The inset to Fig. 2 shows the dependence of the PL signal for Sample A over six orders of magnitude of laser excitation

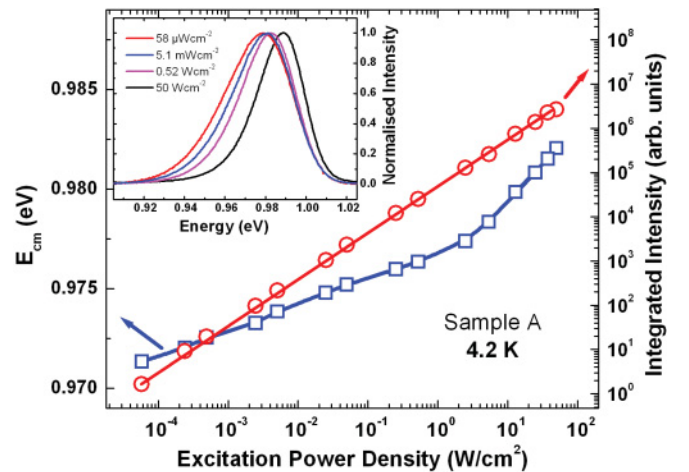


FIG. 2. (Color online) PL energy (squares) and integrated intensity (circles) as a function of excitation power density for Sample A. A clear blueshift is observed, hinting at spatially indirect recombination. The integrated intensity is linearly dependent on the excitation power, confirming that the recombination is excitonic. The excitation power dependence over six orders of magnitude is shown in the inset for Sample A. The blueshift, combined with a reduced importance of the low-energy broadening of the PL peak at high excitation power, is clearly noticeable.

power density. We observe a clear blueshift when increasing the excitation power density, a phenomenon that is commonly attributed to spatially indirect recombination.^{15–17} However, since we are studying type-I two-dimensional structures, a spatial separation of the charge carriers is only possible by means of localized potential fluctuations that can separately trap electrons and holes. Indeed, the blueshift of the PL energy with increasing excitation power has also been attributed to carrier filling of the localized states.¹¹ The PL line shape exhibits a pronounced broadening at the low energy side, revealing the presence of localized band tail states.^{11–13,18,19} The signal becomes increasingly Gaussian at higher excitation powers, indicating that the localized recombination centers tend to saturate at higher excitation power densities.^{20,21} Figure 2 depicts the PL energy over six orders of magnitude of excitation power density. The blueshift mentioned above is clearly present. The change in slope at higher power densities is a consequence of plotting E_{cm} versus laser power semilogarithmically. Note that the integrated intensity of the PL signal shows an entirely linear dependence on excitation power as is expected for luminescence originating from single excitonic recombination.²²

One reason for supposing that higher excitation power densities fill up the localized states can be found when investigating the T dependence of the PL energy at different excitation powers. Figure 3 shows that the excitation-power-induced blueshift for Sample A is strongly T dependent, in such a way that an increase in excitation power density progressively suppresses the typical S-shaped T dependence of the PL energy. While at low excitation power, a local minimum with a depth of about 15 meV is observed, the T dependence measured at the highest excitation powers accessible with our setup recovers to a nearly band-gap-like behavior. However, the explanation that suppression of the S shape is a result of filling of localized states is not consistent with the magneto-PL data discussed below, and we are forced to conclude that

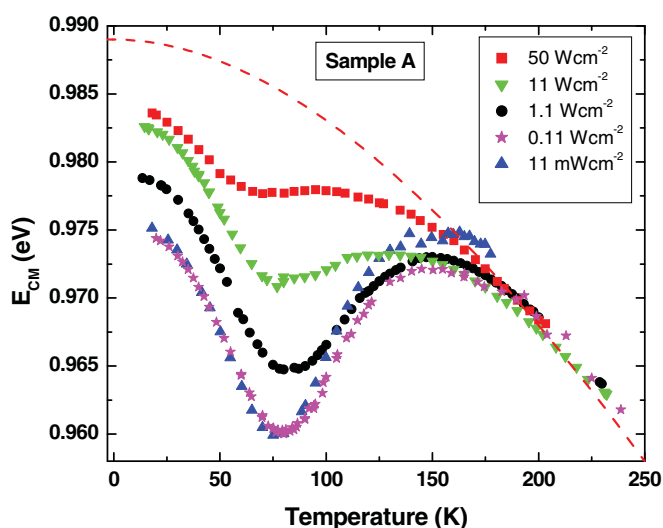


FIG. 3. (Color online) Temperature dependence of the PL energy for Sample A at different excitation power densities. The local minimum in the S shape of the temperature dependence is increasingly suppressed at higher excitation power densities. The dashed line is the Varshni fit from Fig. 1.

the laser-induced blueshift is essentially due to separation of electrons and holes. Finally, Fig. 3 shows that the blueshift found at lower temperatures is absent for $T > 150$ K.

PL studies with varying excitation powers for Sample B reveal a completely different result. Within the experimental errors, there is no detectable shift of the PL peak for laser power densities increasing over five orders of magnitude (not shown). Since the integrated intensity is characterized by a linear scaling to the excitation power, similar to the situation in Sample A, we conclude that the recombination in Sample B is also from single excitons, but that the absence of the excitation power-dependent blueshift demonstrates a considerable reduction in the localization of the charge carriers. It is probable that the shallow hole localization potential is more easily screened than in Sample A, and the expected blueshift is undetectable.

Magneto-PL experiments give a more microscopic picture of the carrier localization in our samples. The inset of Fig. 4 shows the raw PL spectra for both Samples A and B at 0 and 48 T measured at 4.2 K with an excitation power density of 5 Wcm^{-2} . The low-energy broadening, which is a typical manifestation of recombination originating from localized excitons and is commonly observed in $\text{Ga}_{1-x}\text{In}_x\text{N}_y\text{As}_{1-y}$ QWs,^{11–13,18,19} is present in the spectra of Sample A only, not Sample B. Additionally, it can be seen that the line width, measured as the full width at half maximum (FWHM) of the PL signal, is significantly reduced going from Sample A to Sample B (from 31 to 22 meV, respectively). The observed inhomogeneous broadening is the result of compositional and structural disorder, which is inevitably present in these quaternary structures,²³ and hence is a reliable parameter to judge the optical quality of our multiple quantum well (MQW) samples. The suppression of the low-energy broadening and the decrease of the line width by about 30% when going from Sample A to Sample B confirm that a lower growth temperature and the incorporation of indium in the barrier material (Sample B only) have a positive effect on the optical quality of $\text{Ga}_{1-x}\text{In}_x\text{N}_y\text{As}_{1-y}$ MQW structures.^{6,9} We should note that apart from a low-energy broadening in Sample A, a high-energy feature is present in the PL signal of Sample B only. Very little is known up to now about its origin, but we have found that the feature does not exhibit a shift in energy as a function of either excitation power or temperature (not shown here), suggesting that it cannot be due to free-exciton recombination. In contrast, we do observe a shift of this feature with magnetic field (inset of Fig. 4), excluding the possibility that it is a trivial artifact related to the experimental setup.

Figure 4 shows the shift of the PL energy ΔE_{cm} versus magnetic field for both samples A and B at 4.2 K. The center of mass of the PL peak of Sample B is characterized by a linear dependence on magnetic field right down to the very lowest fields that can be produced with our pulsed fields setup, whereas the data for Sample A show a crossover from parabolic to linear behavior at around $B_c = 8$ T, indicating that for Sample A, a stronger magnetic field is required to reach the high-field regime. This shows that the exciton wave functions in Sample B, which has indium in the barriers and is grown at lower T , are substantially more extended than for Sample A at these low temperatures. The spatial extent of

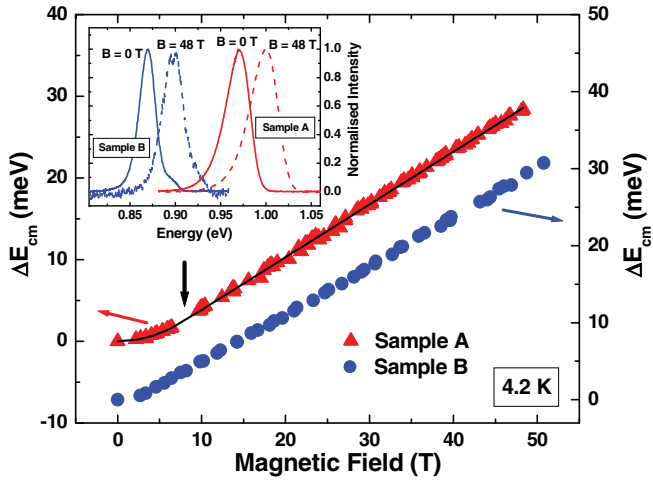


FIG. 4. (Color online) The shift of the PL energy versus magnetic field at a power density of 5 Wcm^{-2} . The line is a fit to the data of Sample A using the model of Ref. 10. For Sample A, a crossover from parabolic to linear behavior occurs at 8 T (indicated by the vertical arrow), whereas the data for Sample B are linear down to very low fields. The inset shows the PL spectra for both samples A (red) and B (blue) at 0 (full lines) and 48 T (dotted lines) measured at 4.2 K. The low-energy broadening is present in the data for Sample A only. The line width of the PL peak for Sample B is considerably smaller.

the wave function for an unconfined exciton is related to its effective mass through the Bohr radius

$$a_B = \frac{0.529\varepsilon}{\mu/m_0} \text{Å}, \quad (2)$$

where ε is the dielectric constant, μ is the reduced exciton mass, and m_0 is the mass of the free electron. Thus, a plausible reason to account for the change in the exciton wave function extent is a decrease in μ when going from Sample A to Sample B. However, we do not expect large differences in mass for these nitrogen concentrations,²⁴ and the data in Fig. 4 show an almost identical slope of the E_{cm} versus B curve in the high-field regime, suggesting no difference in μ between Samples A and B.¹⁰ Hence, the change in exciton wave-function extent derived from the difference in magneto-PL at the lowest fields cannot be explained in terms of a change in effective mass. Since the magneto-PL experiments were performed at very low T , we are measuring recombination between electron-hole pairs for which at least one carrier is localized, i.e. recombination from localized excitons. We therefore propose that the reduced exciton wave-function extent measured in Sample A is related to the localization effects already identified in the T dependence of E_{cm} (see Fig. 1). At this stage, the data indicate that the localization keeps the carriers further apart for Sample B than for Sample A.

It is interesting to investigate a possible correlation between the blueshift with increasing excitation power observed in Sample A (see Fig. 3) and an evolution in the exciton effective mass or exciton wave-function extent. Figure 5 shows the PL energy shift versus magnetic field for various excitation power densities at 77 K, the T at which the largest blueshift was observed (see Fig. 3). Again, the same excitation-induced blueshift (in the $B = 0$ PL energy) is clearly identified, but

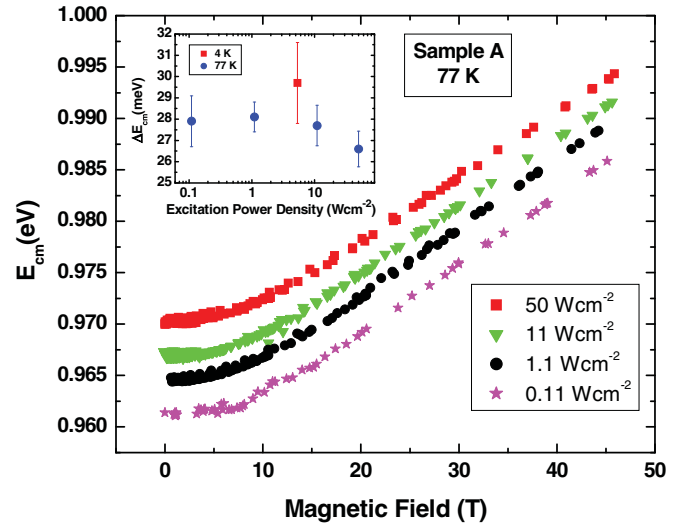


FIG. 5. (Color online) PL energy shift as a function of magnetic field for various excitation power densities at 77 K. The inset shows a summary of the magnitudes of the energy shift between 0 and 45 T for the four different excitation power densities at 77 K and the corresponding energy shift at 4 K. The larger uncertainty in the 4 K PL energy shift is due to fewer data points in the low-field regime for the measurement at this temperature.

there is no change in the magneto-PL. The inset compares the measured PL energy shifts between 0 and 45 T for the four different excitation power densities at 77 K with the shift measured at 4 K. The decrease in energy shift when going to higher temperatures will be discussed at length in the following section, but given the large differences in zero-field PL energy for different excitation powers, it is somewhat surprising that there is no obvious change in the PL energy shift with field when varying the excitation power. This type of behavior has been observed previously for the PL from the wetting layer in GaSb/GaAs quantum dots,²⁵ which as a type-II system is somewhat analogous to the present situation of disorder-induced charge separation. No change in the wetting-layer magneto-PL was observed when increasing the excitation power despite a large blueshift of the zero-field PL energy. In contrast, the magneto-PL for the GaSb quantum dots was found to be dependent on excitation power. The difference in behavior was attributed to the fact that the quantum dots can be multiply occupied with holes, i.e. holes can be forced to occupy the same volume resulting in the formation of exciton complexes, whereas holes in the wetting layer cannot because they just diffuse apart. The blueshift of the PL energy for the GaSb wetting layer is then the result of a collective band (bending) effect, while the magneto-PL still only probes single excitons. We assert that a similar effect is observed in the present system. Correspondingly, both Samples A and B behave similarly in the presence of a magnetic field, as will be pointed out below, while in the absence of field a large blueshift with increasing excitation power is observed for Sample A but is undetectable for Sample B.

Although the field dependence of Sample B appears linear down to very low fields (see Fig. 4), a small parabolic regime still cannot be completely excluded. Moreover, the longer integration times (>5 ms) required at higher T rule out

the pulsed field technique to perform temperature-dependent magneto-PL experiments on our samples. Given the low magnetic fields at which the crossover between diamagnetic and linear field-dependence behavior occurs, magneto-PL in DC fields up to 12 T has been used to study the carrier localization in both samples in more detail and to help distinguish between the effect of localization on the electrons and the holes.²⁶ From the pulsed field data we have found that the exciton radius at very low temperatures is substantially more extended for Sample B than for Sample A, since we were unable to detect diamagnetic behavior for Sample B. The analysis of the PL energy as a function of DC magnetic field (see inset of Fig. 6) reveals a small parabolic regime in fields up to about 4 T at 5 K for Sample B. Using Eq. (1) we have determined an average value for the exciton wave-function extent of 17.5 nm, larger than the corresponding value for Sample A, which is 14.5 nm.

The inset to Fig. 6 shows that slightly increasing the temperature from 5 to 50 K moves the crossover point between the low- and high-field regime for Sample B to much higher fields but that it does not change much going from 50 to 100 K. Correspondingly, the exciton wave-function extent is characterized by a rapid decrease as a function of temperature, followed by an apparent saturation to a value of 12 nm for $T > 50$ K (see Fig. 6), in agreement with earlier studies.¹⁴ For Sample A, the situation is similar, but less dramatic. At low temperatures, the excitons are more compact than in Sample B (equivalent to what was found in pulsed fields), and a gradual

decrease toward the common value of 12 nm at 200 K is observed.

IV. DISCUSSION

In an effort to understand the behavior we have observed, we will briefly discuss the influence of the growth temperature on the structural and optical quality of $\text{Ga}_{1-x}\text{In}_x\text{N}_y\text{As}_{1-y}$ MQWs as previously studied by various groups.^{27–30} Transmission electron microscopy (TEM) studies performed by Herrera *et al.*^{28–30} indicate that an increase in growth temperature enhances In/Ga interdiffusion during growth, which leads to TEM-observable composition fluctuations in the structure. The phase separation between the group-III elements leads to the coexistence of two independent composition profiles for In and N, which are out of phase.³⁰ The intensity of the TEM contrast is drastically increased when raising the growth temperature, and for samples grown at very high temperatures (460 °C), undulations with a periodicity of 20 nm are observed. The amplitude of the contrast is related to the FWHM of the PL peak in these samples, i.e. the TEM-observed degradation of the structural properties when growing at higher temperatures causes a decrease in optical quality. Additionally, the period of the contrasts observed in TEM is reduced when raising the growth temperature, indicating that the scale of the disorder is larger in the samples grown at lower temperatures, although the amplitude is smaller.

This is entirely consistent with our results. Due to the difference in growth temperature also present in our samples, the composition modulation in Sample B is reduced with respect to that of Sample A, and the length scale of the disorder in Sample B is larger than in Sample A. The introduction of indium in the barrier material of Sample B reduces the strain at the QW-barrier interface, further lowering the inhomogeneity of the $\text{Ga}_{1-x}\text{In}_x\text{N}_y\text{As}_{1-y}$ QWs in the sample.^{6,9} Hence, the effect of carrier localization is expected to be much stronger in Sample A, while the period of the modulation is larger in Sample B. The result is that, in both samples, the electrons may be trapped by nitrogen-rich^{24,31} regions, while the holes may only be localized in In-rich parts of the sample, separating them from electrons in the N-rich regions at low temperatures in an out-of-phase manner (Fig. 7). However, the separation is small enough to still allow recombination, and a measurement of the electron and hole wave-function extent related to the size of the relevant localization potentials is essentially the same as measuring the average distance between the localization centers confining these wave functions. In other words, at low T the electrons and the holes are being localized at different locations by nitrogen- and indium-rich regions, respectively, but the separation is larger in Sample B, which was grown under optimized conditions, compared to Sample A. Our results clearly corroborate the localization picture as established by TEM in similar samples.^{27–30} the spatial separation between the electrons and the holes imposed by the disorder-induced local minima in the potential profile is more pronounced in the sample grown at lower temperature due to the increase in the period between composition modulations. In contrast, the activation energy required to free the carriers and recover the free-exciton wave-function extent is smaller than in the samples grown at

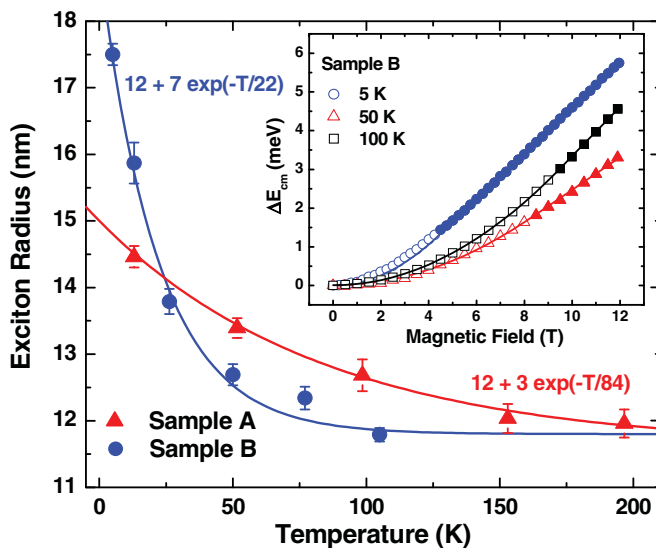


FIG. 6. (Color online) Exciton wave-function extent as a function of T for the DC-field measurements using 2.5 Wcm^{-2} of excitation power. At low T , the exciton radius in Sample B is larger than in Sample A, but as T increases, the relation rapidly reverses. The lines are unconstrained exponential fits to the data. The PL energy shift as a function of DC magnetic field for Sample B at 5, 50, and 100 K is shown in the inset. The open symbols represent data points in the low-field regime, while filled symbols are used for data points at magnetic fields above the crossover point, i.e. in the high-field regime. In contrast to the pulsed field data, a small parabolic regime can clearly be observed.

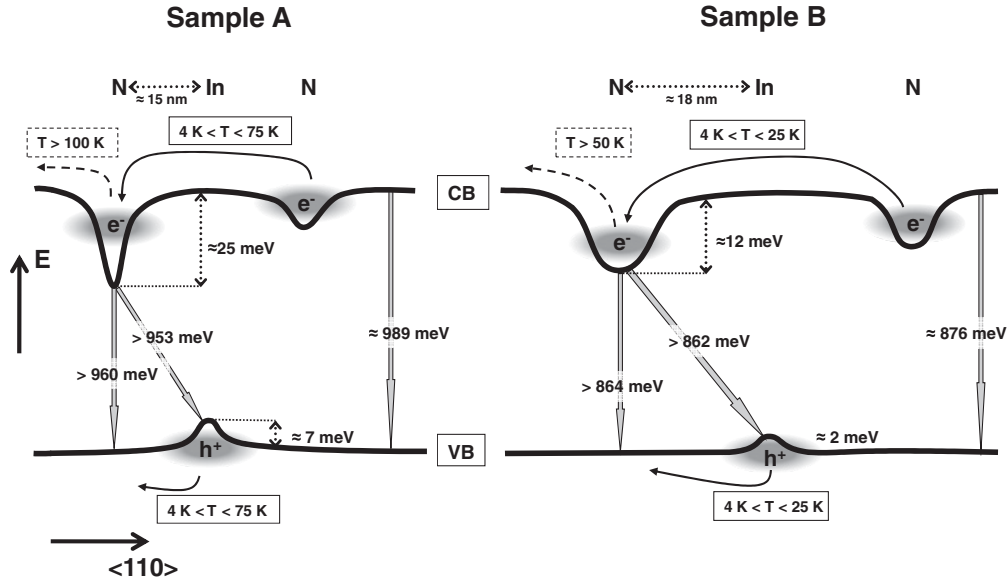


FIG. 7. Schematic representation of the potential landscape based on our observations. The electron and hole localization centers, due to local nitrogen and indium excess, respectively, are expected to be present in an out-of-phase spatially periodic manner (see e.g. Ref. 30). For clarity, the localization centers in the conduction band due to local indium excess are not shown. Recombination energies in the figure are derived from PL center of mass transition energies and are approximate. The average separation of N-rich and In-rich regions is estimated from our data as being 15 nm for Sample A and 18 nm for Sample B.

higher T due to the shallower localization potentials: Sample B, which was grown at 325 °C, exhibits a larger excitonic wave-function extent (spatial separation of electrons and holes) at low temperatures (~ 18 nm from Fig. 6), but this is more rapidly thermally quenched than the Sample A, which was grown at 460 °C (separation of ~ 15 nm).

Between 5 and 50 K, the exciton wave-function extent for Sample B drops by about 30%, while the decrease is only about 7% for Sample A over the same T range, indicating that for Sample B, the detrapping occurs at lower temperatures, in agreement with the zero-field PL energy dependence on T (see Fig. 1). Thermal excitation of the holes from potential fluctuations due to local indium-rich regions into the continuum shifts the nature of the dominant recombination from spatially indirect at low T to direct, hence reducing the exciton radius (Fig. 6). At even higher temperatures, the electrons escape the localization from nitrogen-rich regions, the PL signal is dominated by recombination from free excitons, and the exciton wave-function extent is nearly T independent at higher temperature. Assuming a simple, thermally activated exponential decay of the exciton wave-function extent toward the free-exciton radius of 12 nm, we obtain an activation energy of 7.3 meV (84 K) for Sample A, while it is only 1.9 meV (22 K) for Sample B, and recover the same asymptotic value of 12 nm for the free-exciton extent in both samples (see Fig. 6).

On these grounds and from the observed activation and PL energies, we can then proceed to construct a phenomenological description of the potential landscape in our samples, as shown in Fig. 7. We can estimate the transition energy between electrons localized in the deepest potentials formed by nitrogen-rich regions and free holes from the lowest local minima in the S-shaped T dependence of the PL energy. Note that in Fig. 3 (Sample A data) this minimum is the same for

the lowest two laser powers, whereas for Sample B it was found to be power invariant. By extrapolating the band gap behavior observed at high T toward 0 K using the empirical Varshni law,³² we estimate the band gap for free excitons to be 989 and 876 meV for samples A and B, respectively.³³ The energy difference between this extrapolation and the observed recombination energy at the local minimum of the sigmoidal zero-field T dependence of E_{cm} gives a rough estimate of the electron localization energy in nitrogen localization centers,³⁴ yielding 25 and 12 meV for Samples A and B, respectively. From the exponential modeling of the decrease in exciton radius as a function of T we estimate the valence band localization energy for the indium fluctuations to be about 7 and 2 meV for samples A and B, respectively. Thus the localization energies are more than twice as large for Sample A as for Sample B. This is further supported by the behavior of the data of Fig. 1, where the temperatures of the maxima and minima also differ by a factor of two for the two samples.

V. CONCLUSIONS

We have investigated the behavior of the excitonic emission for two $\text{Ga}_{1-x}\text{In}_x\text{N}_y\text{As}_{1-y}$ MQW samples under the application of a strong magnetic field and have proposed a microscopic picture of the localization effects that are present in these samples. All our observations confirm that the addition of a small percentage (2.3%) of indium to the barrier material and the lowering of the growth temperature from 460 to 325 °C in Sample B induce a considerable enhancement of the optical quality of the structure. The nonmonotonic temperature dependence of the PL energy is much weaker and occurs at a lower temperature for the higher-quality sample, while magneto-PL experiments evidence an increased electron-hole

separation at low temperatures, confirming the existence and nature of composition modulation observed in earlier TEM experiments on similar samples. Thermal quenching of the exciton radius, as observed in the T -dependent magneto-PL, is attributed to redistribution of the holes from regions with indium-induced local potential minima into the continuum, allowing them to move to regions where electrons are trapped by an excess of nitrogen. As T is further increased, the electrons become free as well, and the PL is dominated by free-exciton recombination. The situation is similar for both samples, but is more dramatic and occurs on a longer length scale for Sample B, which was grown at lower temperature and with strain-relieving indium incorporation in the barrier material. An assessment of the potential profiles for both samples from our data leads to the conclusion that the localization energies

are reduced by at least a factor of two in Sample B. This assertion is further endorsed by the observation that, for the low-quality sample only, an excitation power dependence of the PL signal is found.

ACKNOWLEDGMENTS

We thank Q. D. Zhuang for useful discussions and comments on the experiments and M. Capizzi for a critical reading of the manuscript. This work was supported by the Methusalem Funding of the Flemish Government, the Flemish GOA, the Belgian IAP, the Joy Welch Educational Charitable Trust, and the EuroMAGNET project (Contract No. RII3-CT-2004-506239) of the European Commission. M. Hayne acknowledges support of the Research Councils, UK.

*thomas.nuytten@fys.kuleuven.be

†Present address: Department of Electronic and Electrical Engineering, University College London, Torrington Place, London WC1E 7JE, United Kingdom.

¹J. S. Harris Jr., *Semicond. Sci. Technol.* **17**, 880 (2002).

²A. M. Mintairov, K. Sun, J. L. Merz, H. Yuen, S. Bank, M. Wistey, J. S. Harris, G. Peake, A. Egorov, V. Ustinov, R. Kudrawiec, and J. Misiewicz, *Semicond. Sci. Technol.* **24**, 075013 (2009).

³D. Bisping, D. Pucicki, M. Fischer, S. Höfling, and A. Forchel, *J. Cryst. Growth* **311**, 1715 (2009).

⁴E. P. O'Reilly, A. Lindsay, P. J. Klar, A. Polimeni, and M. Capizzi, *Semicond. Sci. Technol.* **24**, 033001 (2009).

⁵S. R. Bank, H. Bae, L. L. Goddard, H. B. Yuen, M. A. Wistey, R. Kudrawiec, and J. S. Harris Jr., *IEEE J. Quantum Electron.* **43**, 773 (2007).

⁶H. Y. Liu, M. Hopkinson, P. Navaretti, M. Guitierrez, J. S. Ng, and J. P. R. David, *Appl. Phys. Lett.* **83**, 4951 (2003).

⁷H. D. Sun, A. H. Clark, H. Y. Liu, M. Hopkinson, S. Calvez, M. D. Dawson, Y. N. Qiu, and J. M. Rorison, *Appl. Phys. Lett.* **85**, 4013 (2004).

⁸H. Y. Liu, C. M. Tey, C. Y. Jin, S. L. Liew, P. Navaretti, M. Hopkinson, and A. G. Cullis, *Appl. Phys. Lett.* **88**, 191907 (2006).

⁹H. Y. Liu, W. M. Soong, P. Navaretti, M. Hopkinson, and J. P. R. David, *Appl. Phys. Lett.* **86**, 062107 (2005).

¹⁰M. Hayne, J. Maes, S. Bersier, M. Henini, L. Müller-Kirsch, Robert Heitz, D. Bimberg, and V. V. Moshchalkov, *Physica B* **346-347**, 421 (2004).

¹¹A. Polimeni, M. Capizzi, M. Geddo, M. Fisher, M. Reinhardt, and A. Forchel, *Phys. Rev. B* **63**, 195320 (2001).

¹²A. Polimeni, M. Capizzi, M. Geddo, M. Fisher, M. Reinhardt, and A. Forchel, *Appl. Phys. Lett.* **77**, 2870 (2000).

¹³L. Grenouillet, C. Bru-Chevallier, G. Guillot, P. Gilet, P. Duvaut, C. Vanuffel, A. Million, and A. Chevenas-Paule, *Appl. Phys. Lett.* **76**, 2241 (2000).

¹⁴G. Baldassarri Höger von Högersthal, A. Polimeni, F. Masia, M. Bissiri, M. Capizzi, D. Gollub, M. Fischer, and A. Forchel, *Phys. Rev. B* **67**, 233304 (2003).

¹⁵F. Hatami, N. N. Ledentsov, M. Grundmann, J. Bohrer, F. Heinrichsdorff, M. Beer, D. Bimberg, S. S. Ruvimov, P. Werner, U. Gosele, J. Heydenreich, U. Richter, S. V. Ivanov, B. Ya. Meltser,

P. S. Kop'ev, and Zh. I. Alferov, *Appl. Phys. Lett.* **67**, 656 (1995).

¹⁶C. E. Pryor and M. E. Pistol, *Phys. Rev. B* **72**, 205311 (2005).

¹⁷B. Bansal, S. Godefroo, M. Hayne, G. Medeiros-Ribeiro, and V. V. Moshchalkov, *Phys. Rev. B* **80**, 205317 (2009).

¹⁸A. M. Mintairov, T. H. Kosel, J. L. Merz, P. A. Blagnov, A. S. Vlasov, V. M. Ustinov, and R. E. Cook, *Phys. Rev. Lett.* **87**, 277401 (2001).

¹⁹I. A. Buyanova, W. M. Chen, G. Pozina, J. P. Bergman, B. Monemar, H. P. Xin, and C. W. Tu, *Appl. Phys. Lett.* **82**, 3662 (2003).

²⁰Y. Sidor, B. Partoens, F. M. Peeters, J. Maes, M. Hayne, D. Fuster, Y. Gonzalez, L. Gonzalez, and V. V. Moshchalkov, *Phys. Rev. B* **76**, 195320 (2007).

²¹F. Ishikawa, A. Guzmán, O. Brandt, A. Trampert, and K. H. Ploog, *J. Appl. Phys.* **104**, 113502 (2008).

²²K. Matsuda, S. V. Nair, H. E. Ruda, Y. Sugimoto, T. Saiki, and K. Yamaguchi, *Appl. Phys. Lett.* **90**, 013101 (2007).

²³E. D. Jones, A. A. Allerman, S. R. Kurtz, N. A. Modine, K. K. Bajaj, S. W. Tozer, and X. Wei, *Phys. Rev. B* **62**, 7144 (2000).

²⁴A. Polimeni, F. Masia, G. Baldassarri Höger von Högersthal, and M. Capizzi, *J. Phys. Condens. Matter* **16**, S3187 (2004).

²⁵M. Hayne, J. Maes, S. Bersier, V. V. Moshchalkov, A. Schliwa, L. Müller-Kirsch, C. Kapteyn, R. Heitz, and D. Bimberg, *Appl. Phys. Lett.* **82**, 4355 (2003).

²⁶M. Hayne, J. Maes, V. V. Moshchalkov, Y. M. Manz, O. G. Schmidt, and K. Eberl, *Appl. Phys. Lett.* **79**, 45 (2001).

²⁷H. Y. Liu, C. M. Tey, C. Y. Jin, S. L. Liew, P. Navaretti, M. Hopkinson, and A. G. Cullis, *Appl. Phys. Lett.* **88**, 191907 (2006).

²⁸M. Herrera, D. González, M. Hopkinson, P. Navaretti, M. Gutiérrez, H. Y. Liu, and R. García, *Semicond. Sci. Technol.* **19**, 813 (2004).

²⁹M. Herrera, D. González, M. Hopkinson, M. Gutiérrez, P. Navaretti, H. Y. Liu, and R. García, *J. Appl. Phys.* **97**, 073705 (2005).

³⁰M. Herrera, D. González, J. G. Lozano, M. Gutierrez, R. García, M. Hopkinson, and H. Y. Liu, *Semicond. Sci. Technol.* **20**, 1096 (2005).

³¹Since the indium- and nitrogen-rich regions across the sample appear in antiphase (see e.g. Ref. 30), a lowering of the conduction band due to local indium excess will be compensated by the simultaneous relative absence of nitrogen. The effect of nitrogen

incorporation on the conduction band energy is about an order of magnitude stronger than that due to local indium excess, and we can therefore safely consider the nitrogen-rich regions as the dominant localization centers for electrons.

³²Y. P. Varshni, *Physica* **34**, 149 (1967).

³³Note that since there is very little data in the high- T free-exciton regime for Sample A, the Varshni fit for this sample is that of Sample B, shifted up in energy.

³⁴M.-A. Pinault and E. Tournié, *Appl. Phys. Lett.* **78**, 1562 (2001).